Nanoscale

PAPER

View Article Online
View Journal | View Issue

Cite this: *Nanoscale*, 2015, **7**, 6653

^{99m}Tc radiolabelling of Fe_3O_4–Au core–shell and Au–Fe_3O_4 dumbbell-like nanoparticles†

M. Felber and R. Alberto*

Received 13th January 2015,
Accepted 8th March 2015

DOI: 10.1039/c5nr00269a

www.rsc.org/nanoscale

The development of nanoparticle-based dual-modality probes for magnetic resonance imaging (MRI) and positron emission tomography (PET) or single photon emission computed tomography (SPECT) is increasingly growing in importance. One of the most commonly used radionuclides for clinical SPECT imaging is ^{99m}Tc and the labelling of Fe_3O_4 nanoparticles with ^{99m}Tc was shown to be a successful strategy to obtain dual-modality imaging agents. In this work, we focus on gold containing magnetic nanomaterials. The radiolabelling of magnetic Fe_3O_4–Au core–shell and Fe_3O_4–Au dumbbell-like nanoparticles with the $[^{99m}Tc(CO)_3]^+$ fragment is described. The key elements for this ^{99m}Tc labelling approach are novel coating ligands, consisting of an anchor for the Au surface, a polyethylene glycol linker and a strong chelator for the $[^{99m}Tc(CO)_3]^+$ moiety.

Introduction

Over the last decade, magnetic nanomaterials (MNs) have gained a lot of interest in the field of biomedical applications, including imaging, drug delivery, protein purification, and therapy.[1–4] The most commonly used MNs are iron oxide nanoparticles (IONPs), especially as magnetic resonance imaging (MRI) contrast agents for T_2-weighted acquisitions.[5] Although this specific modality has a high resolution, the sensitivity of contrast-enhanced acquisitions is limited.[6] This limitation can be overcome by modifying IONPs with additional components in order to establish dual- or multi-modal imaging agents.[7] In particular, several research groups brought the combination of IONPs with a radiolabel for positron emission tomography (PET) or single photon emission computed tomography (SPECT) into focus. This is mainly due to the fact that PET–MRI scanners for clinical imaging and SPECT–MRI for preclinical imaging have become commercially available and offer, therefore, a platform for novel dual-modality tracers. Moreover, the introduction of a radiolabel and subsequent detection of the emitted γ-photons is a highly sensitive imaging technique with lower dose burden to the patient as *e.g.* hybrid PET–CT or SPECT–CT scanners.

There are three strategies to radiolabel IONPs. One strategy is based on bifunctional ligands with a chelate for the radionuclide and an anchor for the IONP surface. de Rosales *et al.* developed bisphosphonate ligands with a dipicolylamine-chelator for the $[^{99m}Tc(CO)_3]^+$ fragment or a dithiocarbamate-chelator for ^{64}Cu.[8–10] This approach involves initial radiolabelling of the ligands, followed by coating on the IONP surface. Another possibility of radiolabelling IONPs is the covalent attachment of a chelator to the existing coating and subsequent labelling with a radionuclide. This concept was, for instance, carried out with 1,4,7,10-tetraazacyclododecane-1,4,7,10-tetraacetic acid (DOTA) for chelation of ^{64}Cu.[11,12] Intrinsically radiolabelled IONPs, not requiring chelators for the radionuclides, represent the third strategy,[13] achieved for instance by incorporating ^{111}In during the synthesis of IONPs or *via* adsorption of ^{69}Ge, radioactive As oxides or ^{89}Zr on the IONP surface.[14–17] Mareque-Rivas *et al.* showed that the $[^{99m}Tc(CO)_3]^+$ fragment can also be adsorbed on the IONP surface, presumably due to the high affinity to hydroxyl groups on the IONP surface.[18,19]

Herein, we aimed at labelling magnetic Fe_3O_4–Au core–shell and Au–Fe_3O_4 dumbbell-like nanoparticles (NPs) with the $[^{99m}Tc(CO)_3]^+$ moiety. We focused our attention on these nanocomposites due to recent reports showing that the degradation products of IONPs increase free radical production in physiological environments which might lead to cell death.[20] Optimal surface coating is absolutely necessary to avoid degradation. Coating a gold shell on IONPs was described to be a promising approach for achieving the desired stability, although the gold shell is not decisive for the magnetic properties.[21] We synthesized novel bifunctional coating ligands bearing lipoic acid (LA) as an anchor for the gold surface, a

Department of Chemistry, University of Zurich, Winterthurerstrasse 190, CH-8057 Zurich, Switzerland. E-mail: ariel@chem.uzh.ch

†Electronic supplementary information (ESI) available: Analyses of Fe_3O_4–Au core–shell nanoparticles; analyses of Au–Fe_3O_4 dumbbell-like nanoparticles; ^{99m}Tc labelling of Fe_3O_4–Au core–shell nanoparticles; ^{99m}Tc complexes; ^{99m}Tc labelling of Au–Fe_3O_4 dumbbell-like nanoparticles; syntheses coating ligands. See DOI: 10.1039/c5nr00269a

polyethylene glycol (PEG) linker and various chelators for the $[^{99m}Tc(CO)_3]^+$ fragment. In addition, the basic coating ligand structure, consisting of LA and PEG, was coupled to d-biotin as a model for a bioactive molecule. Magnetic Fe_3O_4–Au core–shell NPs were functionalised and radiolabelled. The scope of the LA-based ligands was further evaluated in radiolabelling experiments with Au–Fe_3O_4 dumbbell-like NPs.

Experimental

Materials, characterisation and synthesis of coating ligands

Detailed information and synthetic procedures can be found in the ESI.†

Synthesis of Fe_3O_4–Au core–shell NPs

Fe_3O_4–Au core–shell NPs were prepared in two steps according to a reported procedure with slight modifications.[22] In brief, a mixture of iron acetylacetonate (0.18 g, 0.50 mmol), diphenyl ether (6 ml), oleic acid (0.5 ml, 1.57 mmol) and oleylamine (0.5 ml, 1.00 mmol) was stirred under nitrogen at room temperature for 5 min. 1,2-Hexadecanediol (0.65 g, 2.52 mmol) was added and the temperature increased to 210 °C over the course of 30 min. The black mixture was stirred at this temperature for 120 min. After cooling to room temperature, half of this suspension (3.5 ml) was loaded into a syringe and added to a mixture of gold acetate (0.21 g, 0.55 mmol), oleic acid (0.13 ml, 0.41 mmol), 1,2-hexadecanediol (0.78 g, 3.02 mmol) and oleylamine (0.75 ml, 1.50 mmol) in diphenyl ether (7.5 ml). The temperature was increased to 190 °C over the course of 35 min and the mixture was stirred at 190 °C for 90 min. After cooling to room temperature, ethanol (60 ml) was added and the dark purple precipitate was isolated by centrifugation. Finally, the NPs were dried in a vacuum, redispersed in hexane (~15 mg ml^{-1} NPs) and stored at 4 °C.

Phase transfer of Fe_3O_4–Au core–shell NPs

In a typical procedure, basic coating ligand **1** (25.3 μmol), a chelator containing ligand (**2**, **3** or **4**; 8.4 μmol), d-biotin containing ligand (**5**; 8.4 μmol) and tris(2-carboxyethyl)phosphine (TCEP; 12 mg, 42.1 μmol) were dissolved in methanol (800 μl) and water (50 μl). The mixture was vortexed for 5 min and transferred into a nitrogen flushed glass vial with a magnetic stir bar, sealed with a butyl septa and an aluminium-butyl crimp cap. Fe_3O_4–Au NPs (100 μl of the native hexane solution) were diluted with hexane (700 μl) and overlaid on the methanol phase. The mixture was vigorously stirred at room temperature for 20 min. Over the course of the phase transfer, the originally purple hexane phase became completely transparent while the as-functionalised Fe_3O_4–Au NPs were dispersed in the methanol phase. The hexane supernatant with the hydrophobic coating ligands was removed *via* decantation. After evaporation of methanol, the derivatised Fe_3O_4–Au NPs were dispersed in PBS (1 ml). The purification was performed with a PD-10 column using PBS as the mobile phase. The samples were purified three times. Only the purple coloured fractions were collected and the volume was reduced to 1 ml.

^{99m}Tc radiolabelling of Fe_3O_4–Au core–shell NPs

In general, an aqueous solution of $[^{99m}Tc(OH_2)_3(CO)_3]^+$ (0.5 ml, pH = 7–8, 300–390 MBq) was added to purified Fe_3O_4–Au NPs (1 ml in PBS). The mixture was incubated at 50 °C for 120 min. Radiolabelled NPs were purified with a PD-10 column, whereas 12 fractions (each 0.5 ml) were collected directly after loading the column. The activities of the different fractions were measured with a dose calibrator, the NP containing fractions combined and the radiochemical yield determined.

Synthesis of Au–Fe_3O_4 dumbbell-like NPs

Au–Fe_3O_4 dumbbell-like NPs were prepared in two steps according to a reported procedure with slight modifications.[23] 1,2,3,4-Tetrahydronaphthalene (100 ml) was added to tetrachloroauric acid trihydrate (1.0 g, 2.5 mmol), followed by oleylamine (10 ml, 30 mmol). The orange mixture was stirred for 5 min at room temperature and heated at 65 °C for 5 h. Since the orange mixture did not change to an intense red solution, the temperature was elevated to 115 °C for 10 min. After cooling to room temperature, ethanol (100 ml) was added and the precipitated AuNPs were centrifuged, washed with ethanol, dried and redispersed in hexane (~20 mg ml^{-1}). For the synthesis of dumbbell-like NPs, oleic acid (1.0 ml, 3.0 mmol) in 1-octadecene (20 ml) was heated at 120 °C for 20 min under a flow of nitrogen. $Fe(CO)_5$ (0.15 ml, 1.1 mmol) was added and the yellow solution was stirred at 120 °C for 5 min. Oleylamine (0.5 ml, 1.5 mmol) was added, followed by 1.4 ml of the above AuNP solution. The temperature was increased to 310 °C over the course of 20 min and the solution was stirred at 310 °C for additional 45 min. After cooling to room temperature, the particles were separated by adding isopropanol, centrifuged and washed with isopropanol. Dried NPs were finally dispersed in hexane (~10 mg ml^{-1}) and stored at 4 °C.

Phase transfer of Au–Fe_3O_4 dumbbell-like NPs

In a typical procedure, NPs in hexane (500 μl of the native solution) were transferred to a test tube and the solvent was removed under a stream of nitrogen. A solution of water (2.5 ml), 0.01 M acetic acid (1.5 ml) and 25% tetramethylammonium hydroxide solution (120 μl) was added to the NPs and the mixture was sonicated at 37 °C for 30 min. Coating ligand **7** (80 mg) was added and the mixture was sonicated for additional 30 min. After evaporation of the solvent, the black crude was redispersed in PBS (1.5 ml) and purified with a PD-10 column (PBS as the mobile phase) to remove the unbound coating ligand. Purified NPs were kept in PBS at 4 °C.

^{99m}Tc radiolabelling of Au–Fe_3O_4 dumbbell-like NPs

In the first step, chelator containing ligands (**2**, **3**, **4** or **6**) were radiolabelled. An aqueous solution of $[^{99m}Tc(OH_2)_3(CO)_3]^+$ (0.5 ml, pH = 7–8, 170–350 MBq) was added to a ligand solution (0.5 ml, 0.1 mM in water) and the mixture was stirred

at 70 °C for 30 min. Reaction control was carried out with HPLC (trifluoroacetic acid (TFA)–methanol, C18rp). In the second step, a NP solution in PBS (0.5 ml) was mixed with ^{99m}Tc complex solution (0.5 ml) and aqueous TCEP solution (0.5 ml, 1 mg ml^{-1}). The mixture was incubated for 60 min at 50 °C. Radiolabelled NPs were purified as described for radiolabelled Fe_3O_4–Au core–shell NPs.

Results and discussion

Synthesis of bifunctional coating ligands

For efficient and persistent NP labelling, the bifunctional ligand design has to meet several requirements: strong binding to the gold surface, strong chelation to the [^{99m}Tc-(CO)$_3$]$^+$ moiety, high colloidal stability and facile syntheses. Studies showed that LA in its reduced form meets the criteria of strong gold–thiol binding and allows coupling to a linker *via* amide bond formation.[24] As a linker, we chose tetraethylene glycol because it is water soluble, cheap and the terminal hydroxyl groups are easily converted into amines in a three step synthesis (ESI,† section 8).[25] One terminal amine of the linker was protected with *tert*-butoxycarbonyl (boc) and the chelators were generated at the second amine through direct reductive N-alkylations with the corresponding aldehydes (2-pyridinecarboxaldehyde or ethyl glyoxylate).[26] After deprotection of the boc-group, the linker was conjugated to mesyl-LA.[27] Ligand **2** was directly obtained after this step, whereas **3** and **4** required basic hydrolysis of the ethyl ester (Scheme 1). Since we did not intend to coat the NPs quantitatively with the chelator containing ligands, we synthesised compound **1** as a basic coating ligand with a terminal methyl ether, which is known to provide high colloidal stability.[9] Moreover, we covalently attached the LA-PEG-NH_2 moiety to *N*-hydroxysuccinimide activated D-biotin in order to introduce a biomolecule (ligand **5**). We emphasize that basically any bioactive molecule or targeting function with a free carboxylic acid can be introduced at this point.

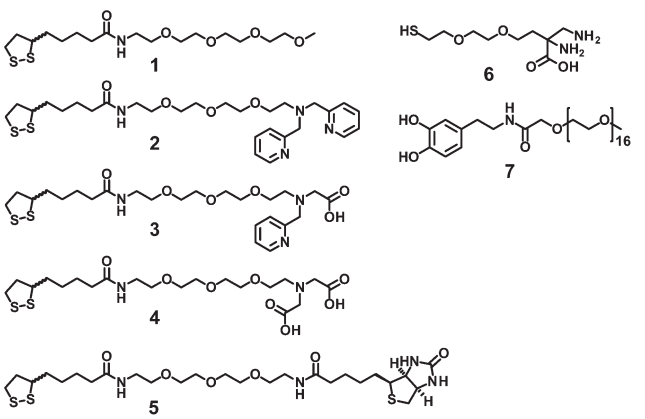

Scheme 1 Overview of the ligands **1–7**.

For the experiments with Au–Fe_3O_4 dumbbell-like NPs we additionally synthesised the 2,3-diaminopropionic acid (DAP) based coating ligand **6** with a monothiol anchor for the gold surface, a ligand system that has been recently introduced by our group.[28] The dopamine derivative **7** was synthesised as a coating ligand for the iron oxide surface of heterostructured Au–Fe_3O_4 dumbbell-like NPs. It is well known that catechols are excellent ligands for Fe_3O_4 surfaces and conjugation to PEG yields in highly stable probes while maintaining the magnetic properties.[29,30]

Synthesis and phase transfer of Fe_3O_4–Au core–shell NPs

Gold shells around the IONP core can be formed using two approaches: directly on the IONP surface[31–37] or onto a middle layer, consisting of silica or a polymer which serves as a bridge between the IONP core and the gold shell.[21,38–44] We synthesised NPs with the gold shell directly on the IONP core according to a reported procedure.[22] Transmission electron microscopy (TEM) analysis of the as-synthesised IONPs showed an average diameter of 5.2 ± 0.4 nm. After the addition of a gold shell, the average diameter was 7.9 ± 0.4 nm, suggesting an average Au shell thickness of ~1.4 nm, which is comparable to the values described in the literature (Fig. 1).[22] The hydrophobic NPs were further analysed by energy dispersive X-ray spectroscopy (EDX). The spectrum exhibited the characteristic peaks for Fe and Au (ESI, Fig. S1†). The Fe and Au concentrations (16 mM and 42 mM) in the hexane solution of hydrophobic core–shell NPs were determined by inductively coupled plasma mass spectrometry (ICP-MS) and the Fe/Au ratio is in the range of the data in the literature.[45]

A crucial step towards water soluble NPs is the transfer from the organic phase to the aqueous phase by replacing the hydrophobic coating with the LA-based ligands. For this we pursued a biphasic approach with the NPs in hexane on the top of a methanol phase containing the hydrophilic ligands. Before addition of the hexane phase, the disulfide of the LA moiety was reduced upon vortexing a mixture of the reducing agent tris(2-carboxyethyl)phosphine (TCEP) and the ligands in methanol. After vigorous stirring for 20 min, the hexane phase became completely colourless, indicating successful functionalisation. After evaporation of methanol, the hydrophilic core–

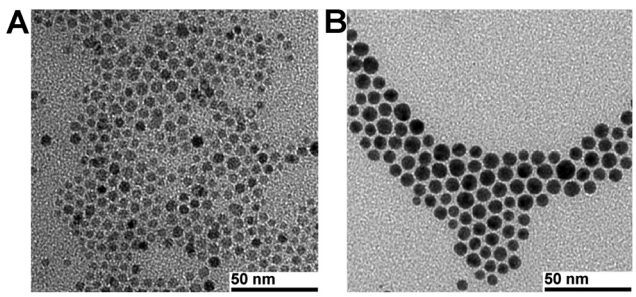

Fig. 1 Representative TEM micrographs of (A) Fe_3O_4 NPs of 5.2 ± 0.4 nm and (B) Fe_3O_4–Au core–shell NPs of 7.9 ± 0.4 nm.

shell NPs were redispersed in phosphate buffered saline (PBS) pH 7.4. A threefold excess of the basic coating ligand **1** relative to the other ligands resulted in highly water soluble NP conjugates. NPs coated with **1** and **2** (3 : 1 ratio) or **1**, **2** and **5** (3 : 1 : 1 ratio) started to precipitate after 1 h, indicating insufficiently high hydrophilicity of these particular NPs with the pyridine groups. However, once carboxylic acids were part of the coating ligands, the derivatised NPs remained highly soluble. In order to remove excess coating ligands and oxidised TCEP the NPs were purified with a PD-10 size exclusion column (Sephadex G-25 medium, PBS as the mobile phase).

This purification step is necessary for radiolabelling experiments since free ligands would compete with ligands attached to the NPs and, hence, lower the radiochemical yields. DLS measurements of the purified NP conjugates showed a hydrodynamic diameter (HDD) of 11 nm when coated with **1** and **3** (3 : 1 ratio), as well as with **1** and **4** (3 : 1 ratio, ESI, Fig. S3 and S4†). With the D-biotin containing ligand **5**, both HDDs increased to 13 nm (ESI, Fig. S5 and S6†). The HDD values did not change after storage at 4 °C for two weeks and at room temperature for one week, demonstrating the high colloidal stability of these NPs. The surface plasmon resonance (SPR) band was found to be at 547 nm for hydrophobic and hydrophilic NPs, which is consistent with the values described in the literature (ESI, Fig. S2a and S2b†).[22]

Synthesis and phase transfer of Au–Fe_3O_4 dumbbell-like NPs

Heterostructured dumbbell-like NPs were synthesised according to the procedure developed by Sun *et al.*, comprising the formation of AuNPs in the first step and the decomposition of iron pentacarbonyl on the AuNP surface in the second step.[23] AuNP cores had an average diameter of 10.1 ± 0.6 nm and the as-synthesised Au–Fe_3O_4 dumbbell-like NPs 26.1 ± 1.6 nm (Fig. 2). ICP-MS analysis of the NPs dispersed in hexane revealed an Fe concentration of 38 mM and 29 mM for Au. The SPR band of AuNPs was at 524 nm, whereas dumbbell-like NPs showed a red-shift of 16 nm and a significantly lower absorbance (ESI, Fig. S7†).[23]

For the phase transfer, several methods were carried out: mixing hydrophobic NPs with ligand **7** in $CHCl_3$–DMF under basic conditions[30] or generating a water soluble intermediate coated with 1,2-dihydroxybenzoic acid followed by substitution with **7**.[46] These attempts gave only poorly soluble NP conjugates, assuming that the hydrophobic oleylamine coating on the AuNP surface was still intact and subsequently caused aggregation in aqueous media. Therefore, we used tetramethylammonium hydroxide (TMAOH) which stabilises the IONP surface *via* interactions between $[NMe_4]^+$ cations and adsorbed hydroxide anions.[29] With this method extremely stable Au–Fe_3O_4 dumbbell-like NPs can be obtained.[47] We observed, however, that these NPs did not elute from the PD-10 column, a prerequisite for the radiolabelling experiments. Therefore, we synthesised compound **7** and coating with this ligand was successfully achieved by adding **7** directly after the phase transfer with TMAOH. These NP-conjugates can be readily purified with PD-10 columns. The derivatised dumbbell-like NPs exhibited a HDD of 35 nm and the NPs showed high colloidal stability at 4 °C for two weeks and at room temperature for one week (ESI, Fig. S8†). Particularly noteworthy is the fact that the AuNP surface was not coated with a specific thiol containing ligand at this stage. This allowed us to evaluate a so-called pre-labelling, which means the labelling of the ligands **2**, **3**, **4** and **6** with the $[^{99m}Tc(CO)_3]^+$ fragment, followed by the attachment on the AuNP surface.

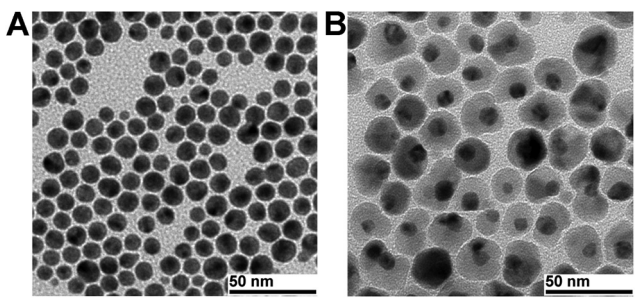

Fig. 2 Representative TEM micrographs of (A) AuNPs of 10.1 ± 0.6 nm and (B) Au–Fe_3O_4 dumbbell NPs of 26.1 ± 1.6 nm (AuNP component appears dark because of the heavy atom effect).

^{99m}Tc radiolabelling of Fe_3O_4–Au core–shell NPs

For the labelling of the core–shell NP conjugates, $[^{99m}Tc(OH_2)_3(CO)_3]^+$ was prepared with an IsoLink™ kit.[48] The three water ligands in $[^{99m}Tc(OH_2)_3(CO)_3]^+$ are labile and can be exchanged with the chelators attached to the NP surface to yield highly robust complexes. Typically, $[^{99m}Tc(OH_2)_3(CO)_3]^+$ in saline was added to NP solutions in PBS (final NP concentration 1 mg ml^{-1}, Fig. 3A, S9A†). Labelling process of NPs can be monitored by HPLC, equipped with a size-exclusion column and two detectors (UV-Vis and γ-counter).[28] Since the radioflow monitors in the γ-counter contain metallic components, we obviously could not apply this method here since the magnetic NPs got stuck to the detector. The HPLC could then not be used anymore until the activity decayed. To avoid this problem, we analysed labelling yields with PD-10 columns by collecting 0.5 ml fractions and measuring the activity in the fractions with a dose calibrator.[9] NPs are found in the first four purple coloured fractions (0.5–2.0 ml) when the column was loaded with a 1.5 ml reaction mixture (Fig. 3B, C, S9B, S9C†). The overall radiochemical yield (RCY) varied from 24% to 52%. NPs coated with ligand **4** gave generally a lower RCY since it is a weaker chelator for the $[^{99m}Tc(CO)_3]^+$ fragment than **3**.[49] A loss of activity during the transfer to the PD-10 column was observed, likely due to non-specific interactions with glass walls and syringe material (Table 1). The D-biotin containing NPs exhibited a lower RCY compared to NPs coated with ligand **1** and chelator **3** or **4** only, consistent with the fact that the gold surface is coated with less chelators in the biotin-coating (20%) than the non-biotin coating (25%). Only 2% of a "blank" $[^{99m}Tc(OH_2)_3(CO)_3]^+$ solution eluted from a PD-10 column, indicating a significantly longer retention of free as

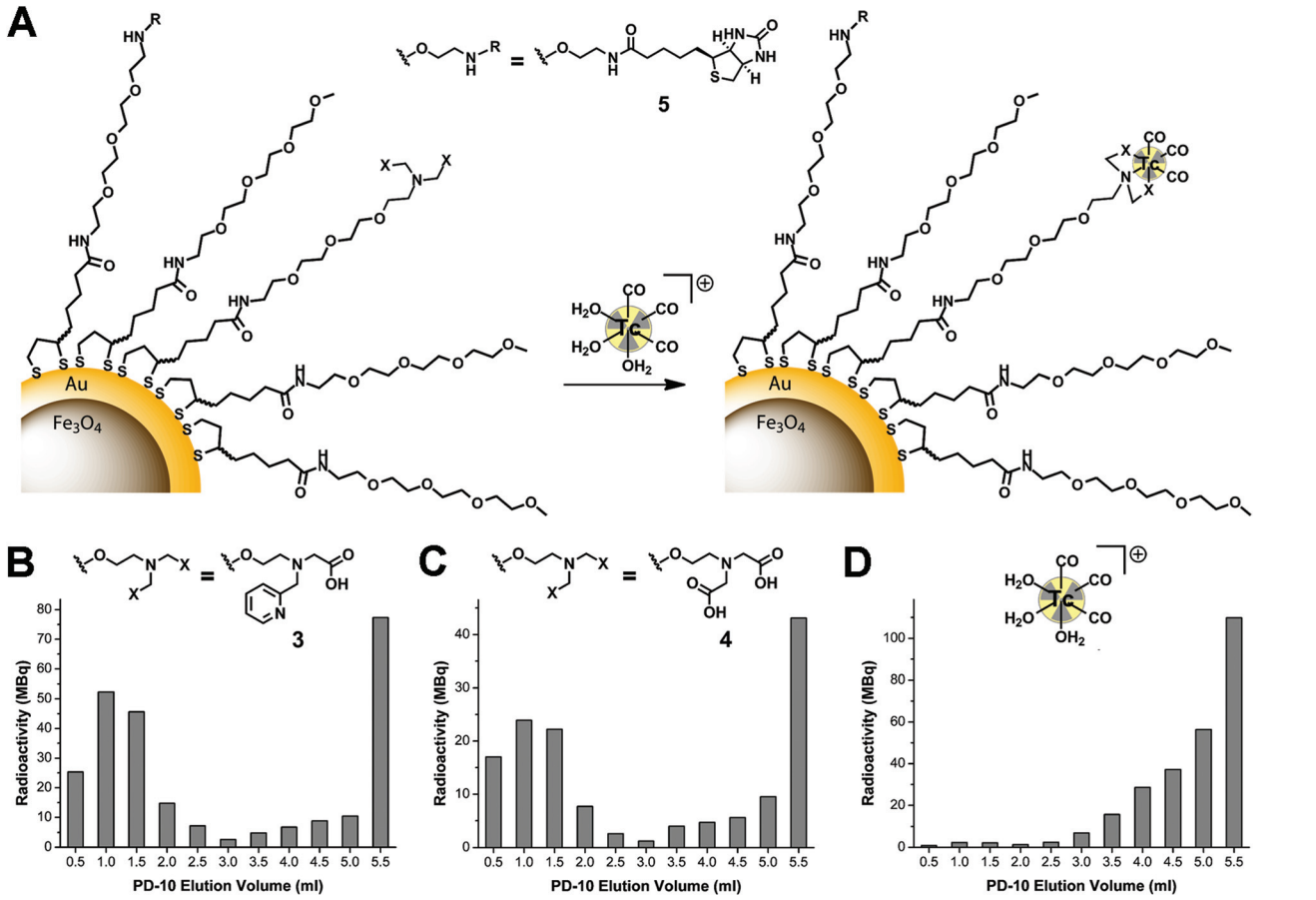

Fig. 3 Radiolabelling of Fe_3O_4–Au core–shell NPs with an illustrative scheme of the labelling procedure (A) and the PD-10 size exclusion chromatograms after incubation at 50 °C for 2 h of NPs containing chelators **3** (B), **4** (C) and a control chromatogram with $[^{99m}Tc(OH_2)_3(CO)_3]^+$ (D). Please note that 0.5 ml fractions were collected and the very last fraction was the remainder activity in the PD-10 column (including the activity in the column). The very first 1.0 ml (two 0.5 ml fractions) is not shown in any of the chromatograms since it always was the mobile phase only.

Table 1 Activity measurements of Fe_3O_4–Au core–shell NP labelling experiments

Coating	Reaction vial[a] [MBq]	PD-10[b] [MBq]	NPs[c] [MBq]	RCY[d]
1, **3**	302	262 (87%)	157	52%
1, **4**	391	338 (86%)	174	45%
1, **3**, **5**	324	263 (81%)	138	43%
1, **4**, **5**	296	146 (50%)	71	24%
Control[e]	427	274 (64%)	6	2%

[a] Activity after incubation at 50 °C for 2 h. [b] Activity loaded on a PD-10 column (in % of total activity). [c] Combined activity from the fractions of 0.0–2.0 ml. [d] Radiochemical yield. [e] Control experiment, 1.5 ml $[^{99m}Tc(OH_2)_3(CO)_3]^+$ loaded on a PD-10 column.

compared to NPs labelled with the $[^{99m}Tc(CO)_3]^+$ fragment (Fig. 3).

^{99m}Tc radiolabelling of Au–Fe_3O_4 dumbbell-like NPs

The dumbbell-like NPs were labelled along a pre-labelling approach. In the first step, ^{99m}Tc complexes of ligands **2**, **3**, **4** and **6** were quantitatively obtained after reacting $[^{99m}Tc(OH_2)_3(CO)_3]^+$ with 0.1 mM ligand solutions at 70 °C for 30 min (Fig. S10–S13†). In the ^{99m}Tc complexes, the disulfides of the LA moieties were reduced by the addition of excess TCEP. Then, the ^{99m}Tc complexes with a mono- or dithiol-anchor for the Au surface were incubated in dumbbell-like NP solution at 50 °C for 60 min (Fig. 4A). Analyses were performed with PD-10 separation and activity measurements of the collected fractions. The RCYs, ranging from 35% to 59%, confirm the ^{99m}Tc pre-labelling approach to be very convenient for dumbbell-like NPs (Fig. 3B–E). The monothiol ligand **6** gave higher yields than the dithiol ligands **2**, **3** and **4** (Table 2), likely caused by the rather quick reoxidation of the dithiol ligands and the concomitant lower affinity to the Au surface. When the ^{99m}Tc complexes were incubated with dumbbell-like NPs without TCEP-reduction, the RCYs were on average 20% lower (Fig. S14 and Table S1†). We also observed that TCEP is necessary for the NP-labelling with the complex containing the monothiol ligand **6**, resulting in 26% higher RCY as compared to labelling without TCEP-reduction. This indicates the presence or formation of disulfides in the absence of TCEP;

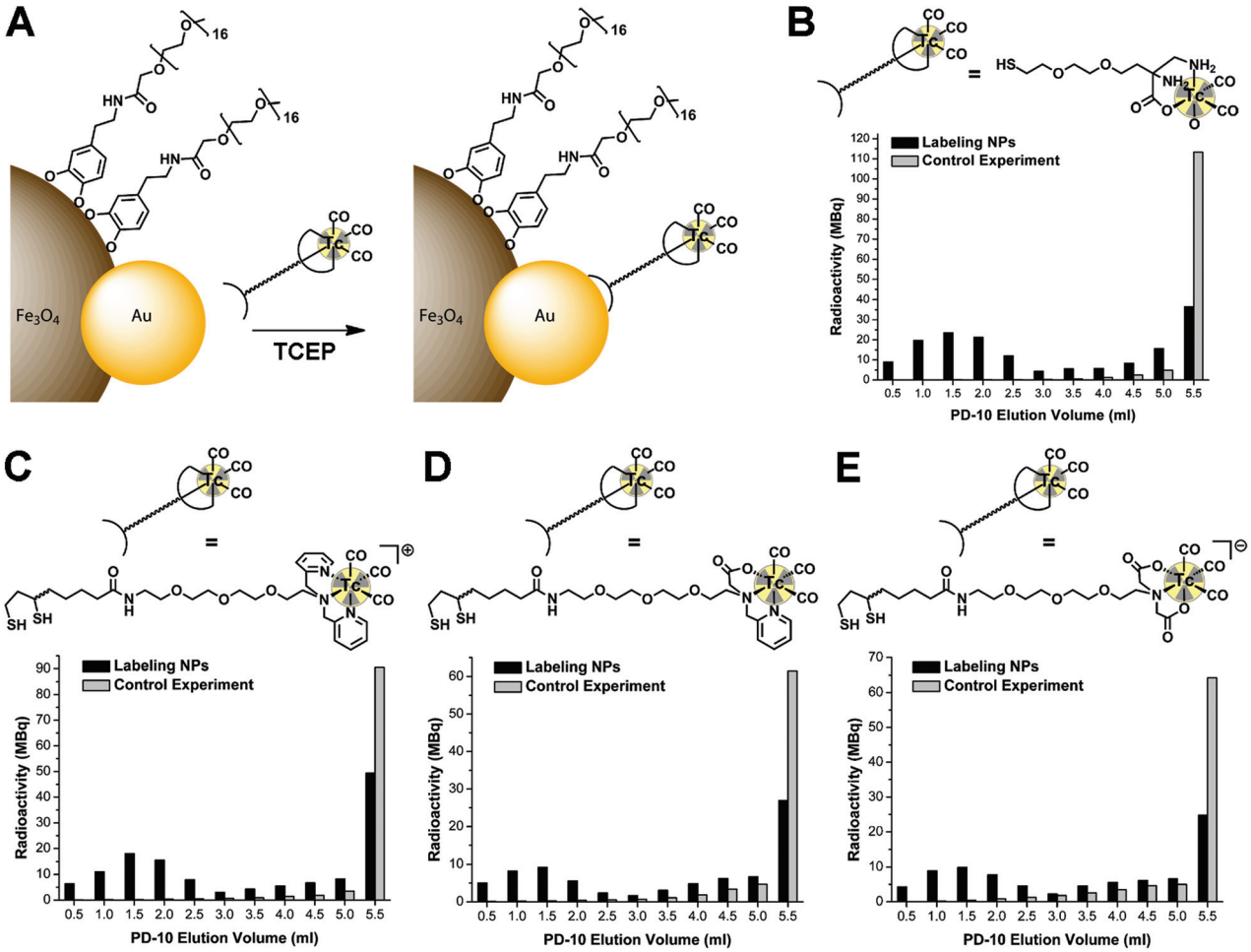

Fig. 4 Radiolabelling of Au–Fe_3O_4 dumbbell-like NPs with an illustrative scheme of the labelling procedure (A) and the PD-10 size exclusion chromatograms after incubation at 50 °C for 60 min of NPs and ^{99m}Tc complexes containing chelators **6** (B), **2** (C), **3** (D), **4** (E) and the corresponding control chromatograms (including reduction with TCEP). Please note that 0.5 ml fractions were collected and the very last fraction was the remainder activity in the PD-10 column (including the activity in the column). The very first 1.0 ml (two 0.5 ml fractions) is not shown in any of the chromatograms since it was always the mobile phase only.

Table 2 Activity measurements of Au–Fe_3O_4 dumbbell-like NP labelling experiments (including reduction with TCEP)

Coating	Reaction vial[a] [MBq]	PD-10[b] [MBq]	NPs[c] [MBq]	RCY[d]
2, 7	157	141 (90%)	59	38%
Control[e]	120	109 (91%)	1	1%
3, 7	87	77 (88%)	30	35%
Control[e]	84	75 (89%)	1	1%
4, 7	86	79 (92%)	35	41%
Control[e]	92	81 (88%)	2	2%
6, 7	144	130 (90%)	85	59%
Control[e]	131	124 (95%)	1	1%

[a] Activity after incubation at 50 °C for 2 h. [b] Activity loaded on a PD-10 column (in % of total activity). [c] Combined activity from the fractions of 0.0–2.5 ml. [d] Radiochemical yield. [e] Control experiments, 1.5 ml ^{99m}Tc complex loaded on a PD-10 column.

however, reoxidation seems to be a minor issue for monothiol ligand **6**. Moreover, compound **6** is less bulky than the LA-derivatives, which in turn leads to higher RCYs.

Conclusions

In this work we demonstrated the feasibility to radiolabel gold containing magnetic nanoparticles with the $[^{99m}Tc(CO)_3]^+$ fragment. On the hand, Fe_3O_4–Au core–shell NPs were labelled using the direct approach, in which the gold surface was coated with bifunctional ligands, consisting of an anchor for the metal surface and chelators for the $[^{99m}Tc(CO)_3]^+$ moiety. On the other hand, Au–Fe_3O_4 dumbbell-like NPs were radiolabelled *via* a pre-labelling strategy; ^{99m}Tc complexes were synthesised first and then coated on the gold surface. Both approaches result in average to good radiochemical yields. These results are the basis for the development of potential, NP-based SPECT/MRI dual-modality imaging agents.

Future work will focus on biological studies (*in vitro* and *in vivo*) with the radiolabelled NP conjugates equipped with cancer-specific targeting vectors to evaluate the applicability for bimodal tumour imaging.

Acknowledgements

We gratefully acknowledge A. Kaech from the Centre for Microscopy and Image Analysis (University of Zurich) for his support throughout the TEM and EDX measurements.

Notes and references

1 J. H. Gao, H. W. Gu and B. Xu, *Acc. Chem. Res.*, 2009, **42**, 1097.
2 Y. W. Jun, J. H. Lee and J. Cheon, *Angew. Chem., Int. Ed.*, 2008, **47**, 5122.
3 J. Gallo, N. J. Long and E. O. Aboagye, *Chem. Soc. Rev.*, 2013, **42**, 7816.
4 C. Tassa, S. Y. Shaw and R. Weissleder, *Acc. Chem. Res.*, 2011, **44**, 842.
5 L. H. Reddy, J. L. Arias, J. Nicolas and P. Couvreur, *Chem. Rev.*, 2012, **112**, 5818.
6 J. V. Jokerst and S. S. Gambhir, *Acc. Chem. Res.*, 2011, **44**, 1050.
7 T. Heidt and M. Nahrendorf, *NMR Biomed.*, 2013, **26**, 756.
8 R. T. M. de Rosales, R. Tavare, A. Glaria, G. Varma, A. Protti and P. J. Blower, *Bioconjugate Chem.*, 2011, **22**, 455.
9 L. Sandiford, A. Phinikaridou, A. Protti, L. K. Meszaros, X. J. Cui, Y. Yan, G. Frodsham, P. A. Williamson, N. Gaddum, R. M. Botnar, P. J. Blower, M. A. Green and R. T. M. de Rosales, *ACS Nano*, 2013, **7**, 500.
10 R. T. M. de Rosales, R. Tavare, R. L. Paul, M. Jauregui-Osoro, A. Protti, A. Glaria, G. Varma, I. Szanda and P. J. Blower, *Angew. Chem., Int. Ed.*, 2011, **50**, 5509.
11 W. B. Cai, K. Chen, Z. B. Li, S. S. Gambhir and X. Y. Chen, *J. Nucl. Med.*, 2007, **48**, 1862.
12 D. Patel, A. Kell, B. Simard, B. Xiang, H. Y. Lin and G. H. Tian, *Biomaterials*, 2011, **32**, 1167–1176.
13 S. Goel, F. Chen, E. B. Ehlerding and W. Cai, *Small*, 2014, **10**, 3825.
14 J. F. Zeng, B. Jia, R. R. Qiao, C. Wang, L. H. Jing, F. Wang and M. Y. Gao, *Chem. Commun.*, 2014, **50**, 2170.
15 F. Chen, P. A. Ellison, C. M. Lewis, H. Hong, Y. Zhang, S. X. Shi, R. Hernandez, M. E. Meyerand, T. E. Barnhart and W. B. Cai, *Angew. Chem., Int. Ed.*, 2013, **52**, 13319.
16 R. Chakravarty, H. F. Valdovinos, F. Chen, C. M. Lewis, P. A. Ellison, H. Luo, M. E. Meyerand, R. J. Nickles and W. Cai, *Adv. Mater.*, 2014, **26**, 5119.
17 E. Boros, A. M. Bowen, L. Josephson, N. Vasdev and J. P. Holland, *Chem. Sci.*, 2015, **6**, 225.
18 N. G. Blanco, M. Jauregui-Osoro, M. Cobaleda-Siles, C. R. Maldonado, M. Henriksen-Lacey, D. Padro, S. Clark and J. C. Mareque-Rivas, *Chem. Commun.*, 2012, **48**, 4211.
19 M. Cobaleda-Siles, M. Henriksen-Lacey, A. R. de Angulo, A. Bernecker, V. G. Vallejo, B. Szczupak, J. Llop, G. Pastor, S. Plaza-Garcia, M. Jauregui-Osoro, L. K. Meszaros and J. C. Mareque-Rivas, *Small*, 2014, **10**, 5054.
20 C. Hoskins, Y. Min, M. Gueorguieva, C. McDougall, A. Volovick, P. Prentice, Z. G. Wang, A. Melzer, A. Cuschieri and L. J. Wang, *J. Nanobiotechnol.*, 2012, **10**, 27.
21 X. D. Wang, H. Y. Liu, D. Chen, X. W. Meng, T. L. Liu, C. H. Fu, N. J. Hao, Y. Q. Zhang, X. L. Wu, J. Ren and F. Q. Tang, *ACS Appl. Mater. Interfaces*, 2013, **5**, 4966.
22 I. Robinson, L. D. Tung, S. Maenosono, C. Walti and N. T. K. Thanh, *Nanoscale*, 2010, **2**, 2624.
23 H. Yu, M. Chen, P. M. Rice, S. X. Wang, R. L. White and S. H. Sun, *Nano Lett.*, 2005, **5**, 379.
24 F. Aldeek, M. A. H. Muhammed, G. Palui, N. Q. Zhan and H. Mattoussi, *ACS Nano*, 2013, **7**, 2509.
25 M. S. Cubberley and B. L. Iverson, *J. Am. Chem. Soc.*, 2001, **123**, 7560.
26 M. K. Levadala, S. R. Banerjee, K. P. Maresca, J. W. Babich and J. Zubieta, *Synthesis*, 2004, 1759.
27 N. Q. Zhan, G. Palui, H. Grise, H. L. Tang, I. Alabugin and H. Mattoussi, *ACS Appl. Mater. Interfaces*, 2013, **5**, 2861.
28 M. Felber, M. Bauwens, J. M. Mateos, S. Imstepf, F. M. Motthagy and R. Alberto, *Chem. – Eur. J.*, 2015, DOI: 10.1002/chem.201405704.
29 E. Amstad, T. Gillich, I. Bilecka, M. Textor and E. Reimhult, *Nano Lett.*, 2009, **9**, 4042.
30 C. Xu, J. Xie, D. Ho, C. Wang, N. Kohler, E. G. Walsh, J. R. Morgan, Y. E. Chin and S. Sun, *Angew. Chem., Int. Ed.*, 2008, **47**, 173.
31 J. L. Lyon, D. A. Fleming, M. B. Stone, P. Schiffer and M. E. Williams, *Nano Lett.*, 2004, **4**, 719.
32 S. J. Cho, B. R. Jarrett, A. Y. Louie and S. M. Kauzlarich, *Nanotechnology*, 2006, **17**, 640.
33 C. J. Xu, B. D. Wang and S. H. Sun, *J. Am. Chem. Soc.*, 2009, **131**, 4216.
34 D. Kim, J. W. Kim, Y. Y. Jeong and S. Jon, *Bull. Korean Chem. Soc.*, 2009, **30**, 1855.
35 M. Kumagai, T. K. Sarma, H. Cabral, S. Kaida, M. Sekino, N. Herlambang, K. Osada, M. R. Kano, N. Nishiyama and K. Kataoka, *Macromol. Rapid Commun.*, 2010, **31**, 1521.
36 J. Salado, M. Insausti, L. Lezama, I. G. de Muro, M. Moros, B. Pelaz, V. Grazu, J. M. de la Fuente and T. Rojo, *Nanotechnology*, 2012, 23.
37 Z. Fan, D. Senapati, A. K. Singh and P. C. Ray, *Mol. Pharmaceutics*, 2013, **10**, 857.
38 Y. Hu, L. J. Meng, L. Y. Niu and Q. H. Lu, *ACS Appl. Mater. Interfaces*, 2013, **5**, 4586.
39 L. Y. Wang, J. W. Bai, Y. J. Li and Y. Huang, *Angew. Chem., Int. Ed.*, 2008, **47**, 2439.
40 W. J. Dong, Y. S. Li, D. C. Niu, Z. Ma, J. L. Gu, Y. Chen, W. R. Zhao, X. H. Liu, C. S. Liu and J. L. Shi, *Adv. Mater.*, 2011, **23**, 5392.
41 J. C. Li, L. F. Zheng, H. D. Cai, W. J. Sun, M. W. Shen, G. X. Zhang and X. Y. Shi, *ACS Appl. Mater. Interfaces*, 2013, **5**, 10357.
42 X. X. He, F. Y. Liu, L. Liu, T. C. Duan, H. M. Zhang and Z. X. Wanq, *Mol. Pharmaceutics*, 2014, **11**, 738.
43 H. D. Cai, K. G. Li, M. W. Shen, S. H. Wen, Y. Luo, C. Peng, G. X. Zhang and X. Y. Shi, *J. Mater. Chem.*, 2012, **22**, 15110.

44 J. C. Li, Y. Hu, J. Yang, P. Wei, W. J. Sun, M. W. Shen, G. X. Zhang and X. Y. Shi, *Biomaterials*, 2015, **38**, 10.
45 L. Y. Wang, J. Luo, Q. Fan, M. Suzuki, I. S. Suzuki, M. H. Engelhard, Y. H. Lin, N. Kim, J. Q. Wang and C. J. Zhong, *J. Phys. Chem. B*, 2005, **109**, 21593.
46 R. Hao, J. Yu, Z. G. Ge, L. Y. Zhao, F. G. Sheng, L. L. Xu, G. J. Li and Y. L. Hou, *Nanoscale*, 2013, **5**, 11954.
47 J. Zhu, Y. J. Lu, Y. G. Li, J. Jiang, L. Cheng, Z. Liu, L. Guo, Y. Pan and H. W. Gu, *Nanoscale*, 2014, **6**, 199.
48 R. Alberto, K. Ortner, N. Wheatley, R. Schibli and A. P. Schubiger, *J. Am. Chem. Soc.*, 2001, **123**, 3135.
49 K. P. Maresca, J. C. Marquis, S. M. Hillier, G. L. Lu, F. J. Femia, C. N. Zimmerman, W. C. Eckelman, J. L. Joyal and J. W. Babich, *Bioconjugate Chem.*, 2010, **21**, 1032.